Journal of Materials Chemistry B

ROYAL SOCIETY OF CHEMISTRY

PAPER

View Article Online
View Journal | View Issue

Cite this: J. Mater. Chem. B, 2020, 8, 10392

Controlled radical polymerization of hydrophilic and zwitterionic brush-like polymers from silk fibroin surfaces†

Danielle L. Heichel, [a] Ngoc Chau H. Vy, [a] Shawn P. Ward, [b] Douglas H. Adamson [ab] and Kelly A. Burke *[acd]

Bombyx mori silk fibroin is a fibrous protein whose tunable properties and biocompatibility have resulted in its utility in a wide-variety of applications, including as drug delivery vehicles, wound dressings, and tissue engineering scaffolds. Control of protein and cell attachment is vital to the performance of biomaterials, but silk fibroin is mostly hydrophobic and interacts nonspecifically with cells and proteins. Silk functionalised with hydrophilic polymers reduces attachment, but the low number of reactive sites makes achieving a uniform conjugation a persistent challenge. This work presents a new approach to grow brush-like polymers from the surface of degradable silk films, where the films were enriched with hydroxyl groups, functionalised with an initiator, and finally reacted with acrylate monomers using atom transfer radical polymerisation. Two different routes to hydroxyl enrichment were investigated, one involving reaction with ethylene oxide (EO) and the other using a two-step photo-catalysed oxidation reaction. Both routes increased surface hydrophilicity, and hydrophilic monomers containing either uncharged (poly(ethylene glycol), PEG) pendant groups or zwitterionic pendant groups were polymerised from the surfaces. The initial processing of the films to induce beta sheet structures was found to impact the success of the polymerizations. Compared to the EO modified or unmodified silk surfaces, the oxidation reaction resulted in more polymer conjugation and the surfaces appear more uniform. Mesenchymal stem cell and protein attachment were the lowest on polymers grown from oxidised surfaces. PEG-containing brush-like polymers displayed lower protein attachment than surfaces conjugated with PEG using a previously reported "grafting to" method, but polymers containing zwitterionic side chains displayed both the lowest contact angles and the lowest cell and protein attachment. This finding may arise from the interactions of the zwitterionic pendant groups through their permanent dipoles and is an important finding because PEG is susceptible to oxidative damage that can reduce efficacy over time. These modified silk materials with lower cell and protein attachments are envisioned to find utility when enhanced diffusion around surfaces is required, such as in drug delivery implants.

Received 16th August 2020,
Accepted 17th October 2020

DOI: 10.1039/d0tb01990a

rsc.li/materials-b

1. Introduction

Silk fibroin from *Bombyx mori*[1] (*B. mori*) is a structural protein that has shown utility for a wide variety of biomaterial applications,[2–4] such as structural implants,[5–7] tissue scaffolds for *in vitro* and *in vivo* use,[8–13] and drug delivery coatings and vehicles.[14,15] One reason for silk's versatility is that control of its molecular weight[16–18] and secondary structure[19–21] (*e.g.*, by exposure to pH changes,[22–24] sonication or vortexting,[25–27] or solvents[28,29]) enable tuning of the material's mechanical properties and stability. Control of protein adsorption and cell attachment to silk is critical to its success in biomaterial applications, but *B. mori* silk fibroin is mostly hydrophobic[30–32] and lacking in specific binding sites for integrins, resulting in the nonspecific attachment of cells and proteins. Though *B. mori* silk materials are often modified to promote interactions with cells and proteins (*e.g.*, by inclusion of natural matrix proteins or ligands for integrins), other applications benefit from reducing these interactions[33,34] such as applications that

[a] Polymer Program, Institute of Materials Science, University of Connecticut, 97 North Eagleville Road Unit 3136, Storrs, CT 06269-3136, USA
[b] Department of Chemistry, University of Connecticut, 55 North Eagleville Road Unit 3060, Storrs, CT 06269-3060, USA
[c] Department of Chemical and Biomolecular Engineering, University of Connecticut, 191 Auditorium Road Unit 3222, Storrs, CT 06269-3222, USA
E-mail: Kelly.Burke@uconn.edu
[d] Department of Biomedical Engineering, University of Connecticut, 260 Glenbrook Road Unit 3247, Storrs, CT 06269-3247, USA

† Electronic supplementary information (ESI) available. See DOI: 10.1039/d0tb01990a

require contact with flowing blood where clot formation and dislodgement are risks for patients. Implanted films and meshes, which can serve as drug delivery surfaces and barriers to support tissues, may also benefit from lower cell and protein attachment to prevent resistance to diffusion[35,36] and to reduce the attachment of surgical adhesions[37,38] that can cause pain, damage surrounding tissues, and increase the complexity of revision surgeries. While chemical modifications of silk have reduced biofouling,[34,39,40] the problem of cell and protein attachment to silk has yet to be solved. This contribution focuses on a new synthetic route to functionalise silk protein films with hydrophilic polymer chains (here referred to as ''brush-like polymers'') of varying composition and determines the impact of the brush-like polymers on cell and protein attachment to degradable films.

Following implantation, biomaterials are rapidly deposited with protein from blood and other fluids, and this protein attachment facilitates the attachment of cells to the surface. Increasing the hydrophilicity of a surface, such as by coupling of poly(ethylene glycol) (PEG), is therefore a well-established approach to reduce cell and/or protein attachment.[41–46] However, both bovine serum albumin (BSA) and human serum albumin (HSA) bind to PEG[47] and the initial deposition of BSA or HSA can enable subsequent cellular attachment to PEGylated surfaces. In addition, PEG and PEG-like surfaces are susceptible to *in vitro* and *in vivo* oxidative damage.[48,49] Zwitterionic polymers (zwitterions contain anionic and cationic groups, but are overall neutral in charge[50,51]) have shown resistance to biofouling in membranes for water treatment.[52,53] We envisioned that a surface layer of brush-like polymers whose repeat units contain zwitterionic pendant groups (side chains) would provide an opportunity to obtain a high density of zwitterions that could interact *via* their permanent dipoles to lower protein and cell attachment to silk surfaces.

Methods to functionalise silk fibroin surfaces with polymer chains can be classified as ''grafting to''[39,54–58] or ''grafting from'',[34,40,59–68] where the former couples a polymer to the surface and the latter grows polymer from the surface.[69] ''Grafting to'' has been used to functionalise silk surfaces with poly(ethylene glycol) (PEG) using cyanuric chloride-functionalised PEG[39] (targets tyrosine residues) to reduce contact angle with water, with alkyne functionalised PEGs[54] (targets tyrosine, histidine, and lysine residues) to reduce attachment of human stem cells and platelets, and with heparin[55] (targets radicals generated on plasma treated surfaces) to reduce blood coagulation and increase cell proliferation on scaffolds. ''Grafting to'' has also been used to functionalise silk solutions with poly(amino acids), for the formation of hydrogels[56] and layer by layer assemblies,[57] and with glycopeptides,[58] for binding of lectins. A recurring challenge with these approaches is that the theoretical number of residues that can be modified is small, therefore there can be a low likelihood that a reactive end of a polymer meets and reacts with a site on the surface. We therefore decided to employ monomers, which have higher diffusion coefficients than polymers, to react with the silk surface and grow brush-like polymers using the ''grafting from'' method.

Silk fibers and fabrics have been modified by ''grafting from'' using free radical polymerisation,[61,62,70] redox polymerisations,[63,64] and controlled radical polymerisations[59,65–68] for textile applications that afford control over wettability[67] or increase flame retardancy and antibacterial properties.[68] Silk biomaterial surfaces have been modified using ''grafting from'' and free radical polymerisation to grow acrylate polymers with 2-methacryloyloxyethyl phosphorylcholine side chains,[40,71] where the resulting surfaces reduced platelet attachment compared to control silk surfaces, and with ferulic acid side chains,[34] where the resulting surfaces increased the whole blood clotting time compared to untreated silk surfaces.[34] Plasma-modified silk surfaces have also been used to grow polymers of poly(2-hydroxymethacrylate) (PHEMA) and poly(acrylic acid) (PAA) by free radical polymerisation, where the PAA brushes were then subsequently modified with poly(ethylene glycol) (PEG, 750 Da) to alter surface hydrophilicity.[60] Though the PAA surface was more hydrophilic than PHEMA, HeLa cells were found to attach in larger amounts to PAA compared to PHEMA and unmodified silk, a finding that may be due to higher amounts of protein adsorbing to the PAA surface. Conjugating PEG to PAA reduced cell attachment to the level of the unmodified silk, but not below. The use of zwitterionic polymers to reduce membrane biofouling, as well as evidence that zwitterions can be used to reduce platelet adhesion,[72] prolong blood clotting,[73] and lower the attachment of proteins to hydrogels to reduce the foreign body response,[74] motivated this study to incorporate zwitterionic moieties on silk materials. While not incorporated into a polymer, a small molecule zwitterion (8-hydroxy-2-octyl phosphorylcholine) was shown to decrease in platelet adhesion[75] to silk surfaces, further supporting this rationale.

This work establishes a new synthetic route to generate brush-like polymers on silk surfaces and to evaluate the ability of polymer surfaces of varying composition to reduce cell and protein attachment. Unmodified silk possesses low amounts of reactive amino acid side chains; therefore, the fibroin films were modified using ethylene oxide or a two-step photo-catalysed oxidation method to overcome silk's few reactive sites, two approaches that are expected to be translatable to other proteins. Brush-like polymers were then synthesized using surface-initiated atom transfer radical polymerisation (ATRP) with two different monomers, one containing a zwitterionic pendant group and the other containing a PEG pendant group. The zwitterionic monomer was selected because its permanent dipoles may promote interactions between neighboring chains, and because it is commercially available with a chemical composition that may be less susceptible to hydrolysis than zwitterionic polymers that employ phosphoester groups.[76] The PEG-containing monomer was selected as an established, uncharged hydrophilic molecule that reduces biofouling and facilitates comparison to the literature. Composition, secondary structure, and surface topography were characterised to elucidate the impact of brush chemistry on the film properties. This work is synthetically distinct from previous

reports of silk films functionalised with polymer chains, which have focused on attaching preformed polymers to the protein (''grafting to'') or polymerising from (''grafting from'') the surface of unmodified or plasma treated silk materials that have a low number of reactive sites. The approach presented results in a greater amount of polymer conjugation, as well as the appearance of a more uniform surface conjugation, that translates into larger reductions of protein and cell attachment to the silk surfaces. Further, these experiments reveal the importance of protein secondary structure (altered *via* film processing) on the success of the polymerisation, which is expected to provide an additional way to tune the reactivity of silk materials in synthetic reactions.

2. Experimental

2.1 Materials

Bombyx mori silkworms were obtained from Tajima Shoji Co., Ltd (Tokyo, Japan). Lithium bromide (LiBr, ≥99%), chloroform (anhydrous, ≥99%), α-Bromoisobutyryl bromide (BIBB, 98%), copper (I) bromide (CuBr, 99.999%), triethylamine (Et_3N, ≥99%), [2-(methacryloyloxy)ethyl]dimethyl-(3-sulfopropyl)ammonium hydroxide (DMAPS, 95%), poly(ethylene glycol) methacrylate (PEGMA, M_n 360), 2,2′-Bipyridyl (bipy, ≥99%), sodium carbonate (Na_2CO_3, ≥99%), sodium bicarbonate ($NaHCO_3$, BioReagent), ammonium persulfate (APS, ≥98%), sodium borate (BioXtra, ≥99.5%) and protease from *Streptomyces griseus* (type XIV) were purchased from Sigma Aldrich (St. Louis, MO). Ethylene oxide (99.9%) was purchased from Praxair (Slatersville, RI). Methanol (ACS certified), Triton X-100 (electrophoresis grade), acetone (ACS certified), regenerated cellulose dialysis tubing (3500 MWCO), Dulbecco's Modified Eagle Medium (DMEM), fetal bovine serum (FBS, qualified), antibiotic–antimycotic (Anti–Anti), CBQCA Protein Quantitation Kit, and phosphate buffered saline (PBS), were obtained from Fisher Scientific (Waltham, MA). CellTiter 96® AQueous One Solution Cell Proliferation Assay (MTS) was purchased from Promega (Madison, WI). Human mesenchymal stem cells (hMSCs) were obtained from Lonza (Walkersville, MD). Methoxypoly(ethylene glycol) activated with cyanuric chloride (mPEG-CC) was purchased from Creative PEGWorks (Chapel Hill, NC). Ultrapure water (dH_2O, 18 Mohm cm) was obtained from an in-house purification unit.

2.2 Experimental methods

2.2.1 Extraction of silk fibroin and film casting. Silk fibroin (SF) was extracted using a previously established protocol.[77] Briefly, 5 g of cut cocoons were boiled in 2 L of 0.02 M Na_2CO_3 for 5 min. The fibers were rinsed with dH_2O three times for 20 min and dried overnight. After drying, the fibers were dissolved in 9.3 M LiBr (5 mL LiBr per gram dry fiber) for 4 h at 60 °C. The resulting solution was dialysed (3500 MWCO) against dH_2O for 48 h, where the water was exchanged 6 times. The impurities of the purified solution were removed by centrifuging at 12 700*g* for 20 min at 6 °C. The typical concentration of the solution obtained was 5 w/v%. For all of the following experiments, the solution was cast into films. The films were fabricated by adjusting the solution concentration to 1 w/v% and applying 500 μL to a polystyrene well (Corning Costar, 1.9 cm^2 area) and allowing to dry overnight, resulting in an ''As Cast'' SF film (denoted here as ''$\mathbf{SF_{As\ Cast}}$'').

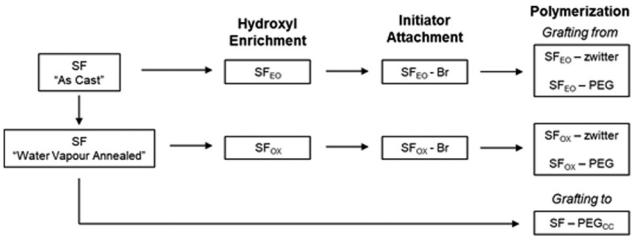

Scheme 1 Flow chart depicting film processing methods and corresponding material compositions.

2.2.2 Enrichment of hydroxyl groups on silk surfaces. To increase the number of reactive groups for the polymerisation, the surface of the SF films was modified to increase hydroxyl content through two different routes, one involving ethylene oxide coupling and the other involving a surface oxidation reaction. A flow chart overview of the synthesis steps is shown in Scheme 1.

2.2.2.1 Ethylene oxide modification. ''As Cast'' SF films ($\mathbf{SF_{As\ Cast}}$) were added to a vacuum reactor before applying an airtight seal. The reactor was degassed under vacuum and vacuum was held for 30 min until a pressure of 10^{-9} to 10^{-10} mbar was obtained. Ethylene oxide (3.2 mL, 64 mmol), which was condensed and dried over calcium hydroxide, was added to the reactor. Then, the reactor was removed from the vacuum line and placed in a 60 °C oil bath, where it was allowed to react for 72 h. The SF films, referred to as ''$\mathbf{SF_{EO}}$'' were removed, rinsed with acetone to remove residual ethylene oxide, and dried at 60 °C for 48 h.

2.2.2.2 Surface oxidation reaction. The photo-catalysed surface oxidation reaction was inspired by a report that modified the surfaces of synthetic polymers.[78] ''As Cast'' SF films ($\mathbf{SF_{As\ Cast}}$) were rendered water-insoluble prior to oxidation *via* water vapour annealing.[19] To water vapour anneal, silk films were dried overnight and transferred to a desiccator that contained liquid water in the bottom of the chamber. The films were suspended above the liquid, and vacuum was generated in the chamber using a water aspirator. After 10 minutes, the chamber was sealed to vacuum, and the films were annealed for 24 h at 25 °C, where the resulting films are denoted ''$\mathbf{SF_{WVA}}$''. Next, 200 μL of 15 w/v% ammonium persulfate (APS) in dH_2O was applied between two $\mathbf{SF_{WVA}}$ films and this layered film assembly was exposed to ultraviolet light (254 nm) for 5 min. This confined film assembly was used to promote the generation of OSO_3^- groups that are hydrolysed to form hydroxyl groups while minimising the formation of carboxylic acid groups.[78] After UV exposure, the films were rinsed with dH_2O to remove excess APS and subsequently incubated in dH_2O for

30 min at 25 °C. The films were then rinsed with acetone for 5 min and water for 5 min, alternating for a total of 3 times in each solvent, before drying at 60 °C for 48 h. These modified films are referred to as "**SF_{OX}**".

2.2.3 Initiator attachment. The modified SF films (**SF_{EO}** or **SF_{OX}**, typical size 1.9 cm^2) were thoroughly dried for 72 h at 80 °C before adding to a round bottom flask that contained anhydrous chloroform (100 mL) and a stir bar. Then, triethylamine (1 mL, 7 mmol) was added to the mixture before purging the vessel with argon for 30 min. α-Bromoisobutyryl bromide (0.25 mL, 2 mmol) was added dropwise to the reaction and the reaction was allowed to proceed for 4 h at 40 °C. The films were thoroughly rinsed with acetone to remove any unreacted reagents and were dried overnight at 60 °C. These films are referred to as **SF_{EO}–Br** if they originated from the ethylene oxide functionalised films and **SF_{OX}–Br** if they originated from the surface oxidised films.

2.2.4 Atom transfer radical polymerisation. Acrylate monomers with two different types of pendant groups were selected to investigate the effect of the brush-like polymer's composition on the surface properties of the films. One monomer contains a poly(ethylene glycol) (PEG) pendant group, where PEG is an uncharged polymer frequently employed to increase hydrophilicity and reduce biofouling. The other monomer contains a zwitterionic pendant group, where the hydrophilic zwitterionic group is charged, yet net neutral.

2.2.4.1 "Grafting from" polymerisation of PEGMA. Copper (I) bromide (CuBr, 15 mg, 0.1 mmol), 2,2′-Bipyridyl (Bipy, 31.2 mg, 0.2 mmol), and initiator attached films (**SF_{EO}–Br** or **SF_{OX}–Br**) were added to a Schlenk tube equipped with a stir bar, and the vessel was purged with argon for 30 min. Poly(ethylene glycol) methacrylate (PEGMA, 0.489 mL, 1.5 mmol) was dissolved in dH_2O/methanol (1 : 4 v : v) and the solution was purged with argon for 30 min before transferring to the Schlenk tube. The polymerisation proceeded for 12 h at 25 °C. The films, denoted as "**SF_{EO}–PEG**" or "**SF_{OX}–PEG**" where the subscript again denotes the hydroxyl enrichment method, were rinsed with methanol and sonicated in dH_2O to remove any bound or unreacted reagents. The films were dried at 60 °C and stored in a desiccator.

2.2.4.2 "Grafting from" polymerisation of DMAPS. Copper(I) bromide (15 mg, 0.1 mmol), Bipy (31.2 mg, 0.2 mmol), and **SF–Br** films were added to a Schenk tube, which was then purged with argon for 30 min. [2-(methacryloyloxy)ethyl]dimethyl-(3-sulfopropyl)ammonium hydroxide (DMAPS, 0.419 g, 1.5 mmol) was added to a solution of dH_2O/methanol (1 : 1 v : v) and was purged with argon for 30 min. The monomer solution was added to the Schlenk tube and the reaction proceeded for 12 h at 25 °C. After polymerisation, the films were rinsed with methanol, sonicated in dH_2O, and dried at 60 °C before storing in a desiccator. The resultant films are denoted as "**SF_{EO}-zwitter**" or "**SF_{OX}-zwitter**" where the subscript denotes the hydroxyl enrichment method.

2.2.5 PEG attachment to silk films by "grafting to". Silk films were cast into wells with an area of 9.6 cm^2 from a 1% w/v solution and allowed to dry overnight. The films were rendered insoluble by water vapour annealing for 24 h at 25 °C. The PEGylation reaction proceeded as previously reported in literature.[39] Briefly, the films were incubated in a solution of 0.02 M sodium borate buffer (pH 9) for 30 min at 25 °C. A solution of methoxypoly(ethylene glycol) activated with cyanuric chloride (mPEG-CC) was prepared at a concentration of 62.5 mg mL^{-1} in 0.02 M sodium borate (pH 9), and 0.998 mL of the solution was added to each silk film. The films were allowed to react with the solution at 4 °C overnight. The product, denoted as "**$SF–PEG_{CC}$**", were rinsed three times with sodium borate buffer to remove unreacted mPEG-CC.

2.3 Characterisation methods

2.3.1 ATR-FTIR. Attenuated total reflectance-Fourier transform infrared (ATR-FTIR) spectroscopy (Magna 560 FTIR spectrometer (Madison, WI) with a diamond ATR accessory (Specac, Fort Washington, PA)) was used to observe changes in functional groups after synthesis and processing steps. After each modification reaction and subsequent drying, the spectra of films were collected by scanning from 4000–400 cm^{-1} (step size 4 cm^{-1}). ATR-FTIR was also used to quantify beta sheets in the films by deconvoluting the Amide I region using Origin software (v. 8.1, Northampton, MA) and established methods.[79]

2.3.2 Contact angle. To quantify the changes in surface hydrophilicity, water contact angle was measured using a sessile drop method (Ramé-Hart goniometer, Mountain Lakes, NJ). After each modification step, the contact angle was measured by depositing a 5 μL drop of dH_2O. Because the **SF-zwitter** films exhibited a very low contact angle from the sessile drop method, the captive bubble method was also used to quantify the contact angle (Pendant Drop Tensiometer, Westbury, NY) of films. The captive bubble measurement was carried out by affixing the films onto a glass slide and placing the slide over a beaker containing dH_2O. Next, an angled needle was used to apply an air bubble with an approximate volume of 20 μL to the film, and the angle between the sample and air bubble was measured.

2.3.3 AFM. Transformations of the silk surface morphology were visualised using an atomic force microscope (AFM) (Asylum Research MFP-3D, Goleta, CA). Samples were dried and mounted onto glass slides with double-sided tape and pressed down using a freshly cleaved mica surface to ensure complete physical contact between the glass slide and the sample. Imaging was performed in tapping (also known as AC) mode using silicon tips (Asylum Probes, AC-160). Scans sizes of 5 × 5 μm were acquired at line rates of 1 Hz, with typical set point and feedback gain settings optimised for surface tracking.

2.3.4 Degradation of films. Unmodified SF films are degradable by hydrolysis or using enzymatic treatments at a rate that has been shown to depend on beta sheet content,[19,21,80] but it was questioned how the addition of brush-like polymers would affect the degradation rate. Films were prepared as described above and dried at 60 °C before beginning the study. The films

were then added to pre-weighed microcentrifuge tubes and 1 mL of 1X PBS (control) or 1X PBS containing 1 U mL^{-1} protease XIV was added to the tube. Every 2 days, the tubes were centrifuged (10 000*g*, 10 min, 25 °C) and the solution was decanted. The films were rinsed with dH_2O and centrifuged again. The water was again decanted and the tubes were allowed to dry for 1 h at 60 °C before measuring the mass. The percent mass remaining, m, at each time point was determined by the formula

$$m = \frac{m_t}{m_o} \times 100$$

where m_t is film's mass at the time measured in the study and m_o is the film's initial mass.

2.3.5 Adsorption of bovine serum albumin. A protein adhesion study was performed to quantify how the synthesis method and chemical composition of the brush-like polymers affect protein attachment to SF films. Larger films were required for this study because the limit of detection of the CBQCA assay. The films were cast by applying 2.5 mL of 1% w/v SF solution to the wells of 6 well plates (9.6 cm^2 per well) and drying at room temperature. The subsequent reactions were carried out as described above to generate the brush-like polymer surfaces. Films were then immersed in 10 mg mL^{-1} bovine serum albumin (BSA) overnight at 6 °C. After incubation, the films were gently washed with 750 μL dH_2O six times to remove loosely attached protein. The films were then incubated with 500 μL of 0.1% v/v Triton X-100 for 1 h at 25 °C to detach the adsorbed BSA. The solutions were collected and assayed with using a CBQCA working solution (2 mM CBQCA in 0.1 M sodium borate). The fluorescence (Ex 465 nm, Em 550 nm) was measured, and BSA was calculated based on a standard curve.

2.3.6 Attachment of human mesenchymal stem cells (hMSCs). The attachment of hMSCs to the silk films was measured using an MTS assay, which detects viable cells using a tetrazolium compound that is reduced into a formazan dye and detected spectroscopically. The films used in this experiment had an area of 0.95 cm^2 but otherwise followed the same synthetic routes described above. Films were sterilised before use by soaking in 70% v/v ethanol for 24 h, rinsing six times with sterile dH_2O, and placing in a sterile 48 well plate. hMSCs (Passage 4) were seeded on the films at a high seeding density (105 000 cells per cm^2). At each time point (1 h, 3 h, 6 h, and 24 h), the films were gently rinsed with 1X PBS to remove any loosely attached cells and transferred to a new sterile 48 well plate. Then, 240 μL of complete medium (89% DMEM, 10% FBS, and 1% anti–anti) and 20 μL of CellTiter 96® AQueous One Solution Reagent (MTS) was added to each well. The samples were incubated for 1 h at 37 °C. Next, 100 μL of the medium was transferred to a 96 well plate, and absorbance at 490 nm was measured with a UV plate reader (BioTek, Winooski, VT). The number of cells attached to films was calculated using a standard curve generated from cells seeded on tissue culture plastic at varying densities.

3. Results and discussion

3.1 Synthesis of polymer brushes on silk fibroin films

Preliminary experiments polymerised the zwitterionic monomer (DMAPS) from the surface of unmodified silk films using atom transfer radical polymerisation (ATRP). These films were methanol annealed, meaning "As Cast" films ($\mathbf{SF_{As\ Cast}}$) were soaked in a 95% methanol/5% water solution for 24 h at 25 °C to induce beta sheets and render the films insoluble in water before reacting with initiator and polymerising with DMAPS, as described in Sections 2.2.3 and 2.2.4.2. The ATR-FTIR spectra of the resulting films showed very low levels of the sulfonate group, indicating that the number of brush-like polymers on the surface of the film and/or the molecular weight of chains was low (Fig. S1, ESI†). We hypothesized that this result may be because the hydroxyl groups in silk fibroin are mostly found in serine residues, which are frequently located in the beta sheet regions of the protein. This motivated us to enrich the hydroxyl content on the film's surface and to use methods that keep beta sheet content in the films low. To keep beta sheet content low, water vapour annealing was used to induce beta sheets instead of methanol[81] annealing, and water vapour annealing was only employed to render the film insoluble for the oxidation reaction (Section 2.2.2.2) because this reaction uses water as a solvent (Scheme 1).[81]

To enrich hydroxyl content, two methods were investigated to modify the surface of SF films. The first method (Scheme 2i) reacted the films with ethylene oxide (EO), which targeted the tyrosine, lysine, serine, cysteine, histidine, and arginine. This product, denoted as "$\mathbf{SF_{EO}}$," has a theoretical degree of hydroxylation of about 18.2 mol%. The second method (Scheme 2ii, a–b) used a surface oxidation method previously reported in literature.[78] The oxidation mechanism is proposed to proceed by abstracting a hydrogen atom from the film's surface to form tertiary SO_4^- groups, which are susceptible to hydrolysis in aqueous media, resulting in the generation of hydroxyl groups[82,83] as well as potentially some carboxylic acid groups. The potential for hydrogen abstraction is dependent on the bond strength, meaning that hydrogens attached to tertiary carbons are more susceptible to abstraction than hydrogens attached to primary carbons. Since this reaction targets surface hydrogen atoms, it has the potential to modify the hydrogen of the amide backbone[84] in addition to the hydrogens attached to tertiary or secondary carbons in the side chains of valine, leucine, isoleucine, proline, methionine, lysine, arginine, glutamine, and glutamic acid residues. In total, these amino acids amount to 5.6 mol% of a silk molecule, but given the reactivity at the hydrogen of the amide backbone, it is difficult to determine a precise theoretical degree of modification of the product, $\mathbf{SF_{OX}}$. Because the number of potential reaction sites for the oxidation reaction, it should be noted that Scheme 2ii, a and b, does not exhibit the full extent of modification.

To confirm successful hydroxyl substitution, the surfaces of the unmodified and modified silk films were characterised using ATR-FTIR (Fig. 1) to assess functional groups and by measuring contact angle with water to characterise surface

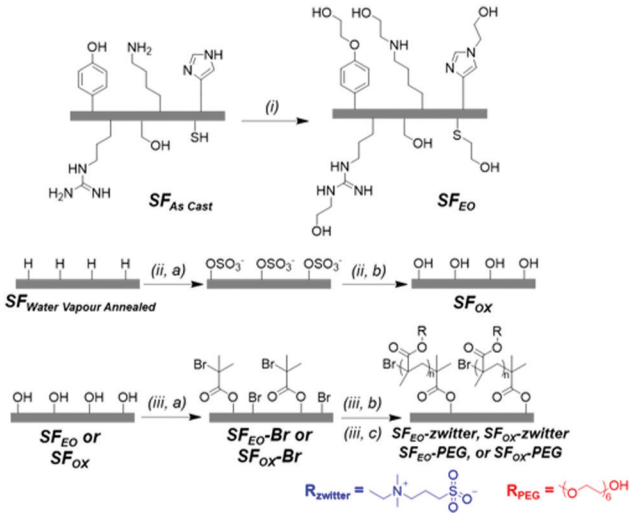

Scheme 2 (i) Ethylene oxide treatment of unmodified silk fibroin (SF) films to result in SF_{EO}; (ii, a) oxidation of unmodified SF films using ammonium persulfate [aqueous 15% w/v APS, 5 min, 25 °C] and (ii, b) hydrolysis of organosulfate groups to hydroxyl groups [dH_2O, 10 min, 25 °C] to result in SF_{OX}; (iii, a) initiator attachment to hydroxylated SF films [NEt_3, BIBB, chloroform, 4 h, 40 °C], (iii, b) ATRP of zwitterionic monomer [CuBr/Bipy, DMAPS, methanol/water, 12 h, 25 °C] and (iii, c) ATRP of PEGMA monomer [CuBr/Bipy, PEGMA, methanol/water, 12 h, 25 °C]. Reaction (ii) has the potential to modify the amide backbone as well as numerous amino acid residues, therefore this scheme is not drawn to show the individual reactive sites that are modified.

hydrophilicity (Fig. 2). The ATR-FTIR spectrum for SF_{EO} (Fig. 1a, Trace ii and b, Trace ii) did not result in the generation of new peaks compared to the unmodified silk surface (Fig. 1a, Trace i and b, Trace i), but the peak from the hydroxyl substitution is expected to overlap with the hydroxyl of the native protein, therefore this result was expected. The ATR-FTIR spectrum for SF_{OX} (Fig. 1a, Trace iii and b, Trace iii) showed the presence of a small peak at $\sim$1740 cm^{-1} due to the formation of carboxyl groups, indicating that some formed despite this being discouraged by the experimental setup, and the signal from the hydroxyl groups was difficult to resolve again due to hydroxyl of the silk film.

To assist in confirming surface modification by EO and by OX methods, the surface hydrophilicity was characterized by contact angle measured using two different methods: sessile drop (Fig. 2a) and captive bubble (Fig. 2b). The unmodified SFs used in the **EO** and **OX** syntheses had different processing methods, where the SF film used in the **EO** synthesis was used "As Cast" ($SF_{As\ Cast}$) and the SF film used in the **OX** synthesis was water vapour annealed (SF_{WVA}) (Scheme 1), which contributes to their different values and is consistent with literature.[81] Compared to the unmodified **SF**, the water contact angle of the hydroxylated films, SF_{EO} and SF_{OX}, decreased (Fig. 2a and b), suggesting that the reaction was successful at increasing hydrophilicity. After modification with **EO**, the contact angle decreased to about 30°, from about 50° for $SF_{As\ Cast}$ (Fig. 2a). This was expected due to the increase in OH groups on the surface, making the film more hydrophilic. Film modification by oxidation also shows a decrease in contact angle to about 30°, which is a significant change from the unmodified SF (SF_{WVA}), which was approximately 65° (Fig. 2a). SF_{EO} and SF_{OX} have similar contact angles, indicating that their surface hydrophilicity is similar.

The modified SFs (SF_{EO} and SF_{OX}) were then reacted with α-bromoisobutyryl bromide (BIBB) to terminate the surface with an initiator suitable for subsequent reactions using atom transfer radical polymerisation (ATRP). To assess successful initiator attachment, ATR-FITR and scanning electron microscopy (SEM, FEI Nova NanoSEM 450, Hillsboro, OR) with energy-dispersive X-ray analysis (EDS, Oxford AZtecEnergy Microanalysis System with X-Max 80 Silicon Drift Detector, Concord, MA)

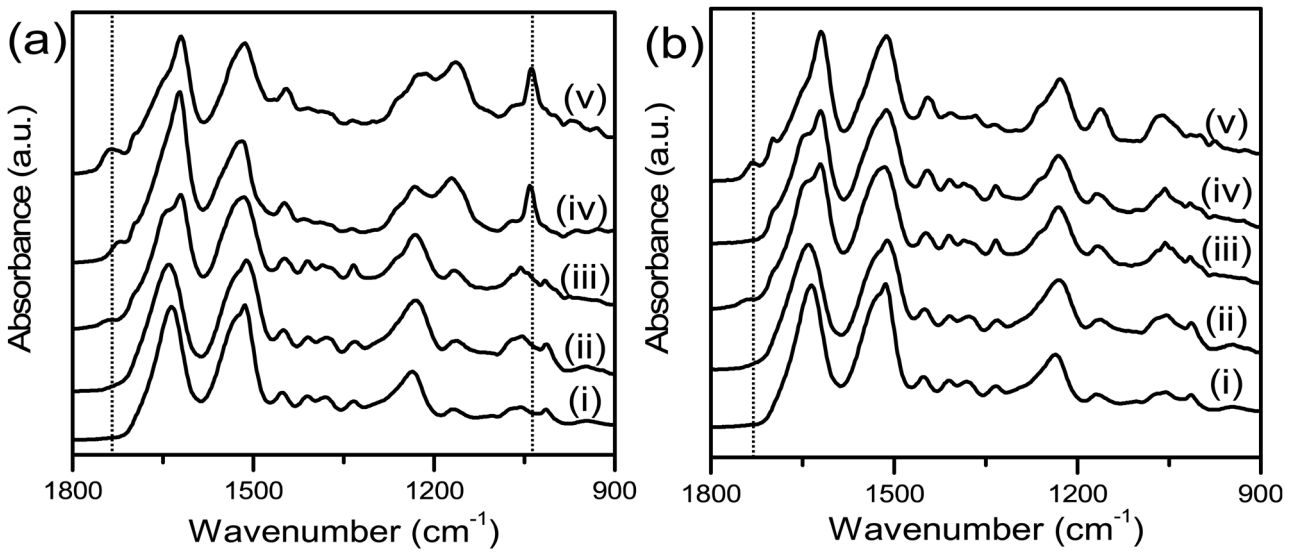

Fig. 1 (a) ATR-FTIR spectra of (i) unmodified SF ($SF_{As\ Cast}$), (ii) SF_{EO}, (iii) SF_{OX}, (iv) SF_{EO}-**zwitter**, (v) SF_{OX}-**zwitter**, and (b) ATR-FTIR spectra of (i) unmodified SF ($SF_{As\ Cast}$), (ii) SF_{EO}, (iii) SF_{OX}, (iv) SF_{EO}–**PEG**, (v) SF_{OX}–**PEG**. Vertical dashed reference lines in (a) correspond to S=O stretching at 1040 cm^{-1} and ester C=O stretching at 1735 cm^{-1}, and the dashed reference line in (b) corresponds to ester C=O stretching at 1735 cm^{-1}.

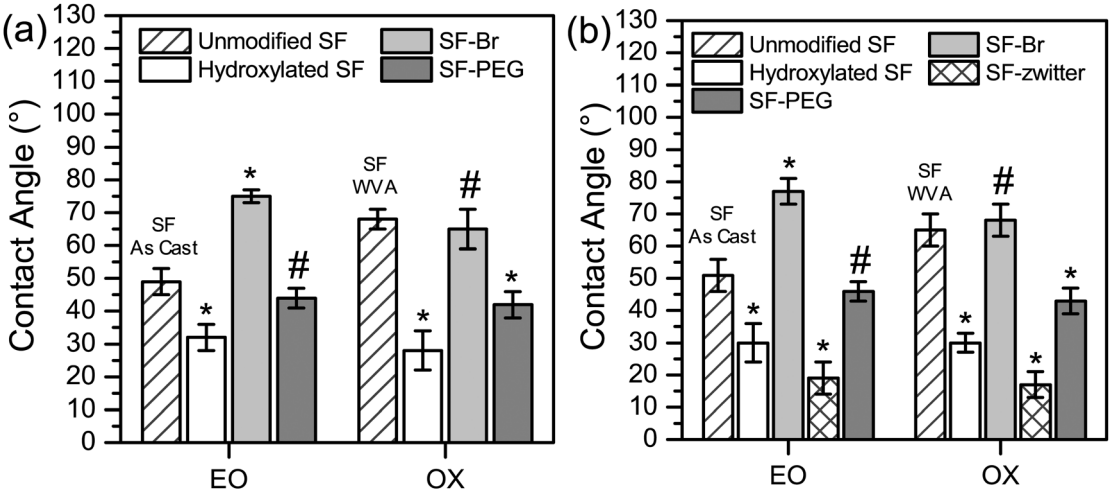

Fig. 2 Water contact angles *via* (a) sessile drop and (b) captive bubble method of unmodified silk, hydroxylated silks, and silk brush films. ''EO'' refers to hydroxyl enrichment by ethylene oxide, and ''OX'' refers to hydroxyl enrichment by photo-catalyzed oxidation. The unmodified SF in ''EO'' series is ''As Cast'' ($\mathbf{SF_{As\ Cast}}$), and unmodified SF in the ''OX'' series was water vapour annealed ($\mathbf{SF_{WVA}}$) to induce beta sheet structures. For (a) and (b), * denotes significance at $p < 0.05$ and # denotes not significant when compared to the unmodified SF within same synthesis group.

(SEM-EDS) were used, but it was found that the C–Br signal in the FTIR spectrum (Fig. S1, ESI†) was obscured by the silk protein signal and SEM-EDS signal was also small compared to the noise (Fig. S2, ESI†). In lieu of direct assay for bromine presence, water contact angle was used to confirm the successful attachment of the initiator. After initiator attachment, the contact angles for **SF–Br** sharply increased from $\sim 30^\circ$ to $\sim 75^\circ$ for the **EO** synthesis and 65° for the **OX** synthesis (Fig. 2a). The change in surface hydrophilicity is consistent with the attachment of hydrophobic initiator.

Using the initiator-attached films, **SF–Br**, polymers were ''grafted from'' the surface of silk by surface-initiated ATRP (SI-ATRP). Two acrylate monomers were selected for investigation. The first contained a poly(ethylene glycol) (PEG) pendant group that is hydrophilic and lacking in charged groups. The second monomer was hydrophilic and zwitterionic, where the charged groups were balanced to obtain an electrically neutral monomer. ATR-FTIR and contact angle were used to confirm successful surface polymerisation of the brush-like polymers. Here, we have chosen to use the term ''brush-like'' to describe the polymers because they are synthesized using the same chemistries that can produce polymer brushes, but a direct measure of surface density of the chains to prove chain interactions was not possible, thus we use the term ''brush-like''. For both $\mathbf{SF_{EO}}$**-zwitter** and $\mathbf{SF_{OX}}$**-zwitter**, the ATR-FTIR spectra (Fig. 1a, Trace iv and v) show a new peak due to the formation of the ester bond from the polymerisation at $\sim$1720–1730 cm^{-1}, and a peak due to the sulfonate ($-SO_3^-$) group of the zwitterionic polymer is present at 1040 cm^{-1}. The amount of sulfonate can be quantified by normalising the amide II region (1500–1600 cm^{-1}) of **SF-zwitter** spectra and determining the area of the sulfonate peak at 1040 cm^{-1}. The areas of $\mathbf{SF_{EO}}$**-zwitter** and $\mathbf{SF_{OX}}$**-zwitter** were 2.29 and 2.45 (relative to the normalised amide II region), respectively, suggesting that the oxidation method results in more brush-like polymer surface functionalization. This result may arise due to the greater number of reactive sites theoretically available to the oxidation reaction compared to the ethylene oxide reaction, though not all reactive sites will generate brush-like polymers because of other constrains, such as sterics. The ATR-FTIR spectra of $\mathbf{SF_{OX}}$**–PEG** and $\mathbf{SF_{EO}}$**–PEG** (Fig. 1b, Trace iv and v) also show the appearance of a peak at 1730 cm^{-1}, indicating successful polymerisation, however the PEG-containing brush-like polymers had no distinct new peaks, hence quantifying by peak deconvolution was not possible.

Because we hypothesized that methanol annealing causes a transformation that reduces the accessibility of reaction sites on SF films, we also ran the photo-catalysed oxidation reaction on films that were annealed by soaking in 95% methanol in water at 25 °C for 24 h. We then attached initiator and attempted ATRP polymerisation of the zwitterionic monomer, but those films were found to display little brush-like polymer content (Fig. S3, ESI†). This supports our hypothesis that the annealing treatments of the silk films impacts their reactivity in these syntheses and validates our approach to use water vapour annealing instead of methanol treatment to render films insoluble prior to hydroxyl enrichment.

The contact angle of PEG-containing brush-like polymer surfaces could be measured using either the sessile drop or captive bubble methods. The zwitterionic-containing brush-like polymer surfaces were found to wet too rapidly to obtain an accurate measurement by sessile drop, therefore only the captive bubble method was used for those films. The contact angles of $\mathbf{SF_{EO}}$**–PEG** and $\mathbf{SF_{OX}}$**–PEG** are shown in Fig. 2a for the sessile drop and Fig. 2b for the captive bubble method, and the values are about 40°, which is a significant decrease from **SF–Br** and shows that the surface was also successfully modified with PEG-containing brush-like polymers. The contact angle for films with PEG-containing brush-like polymers was significantly lower than **SF** when the oxidation method ($\mathbf{SF_{OX}}$**–PEG**)

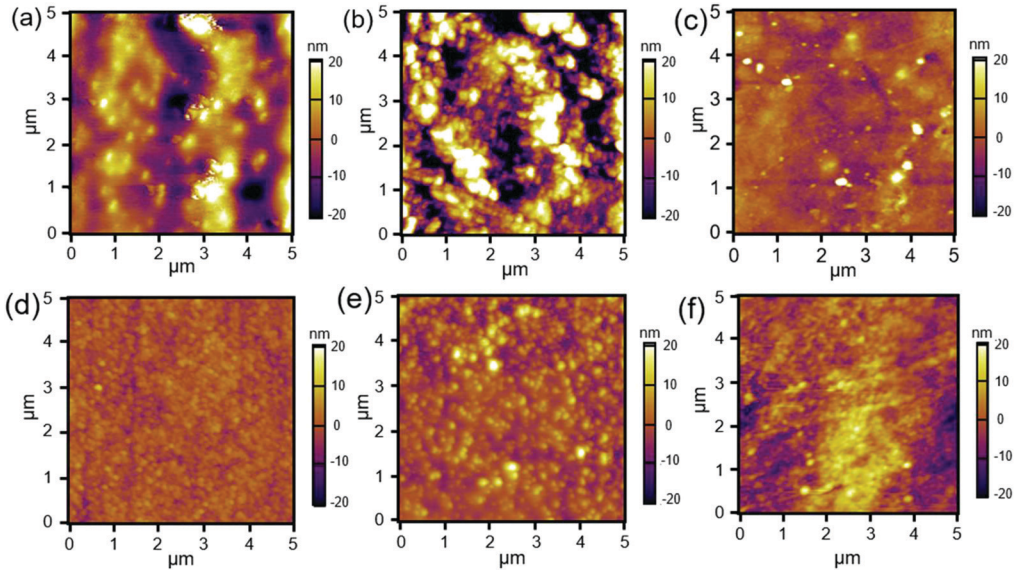

Fig. 3 AFM height micrographs of (a) SF_{EO}, (b) SF_{EO}-zwitter, (c) SF_{EO}–PEG, (d) SF_{OX}, (e) SF_{OX}-zwitter, and (f) SF_{OX}–PEG film surfaces.

was employed, but this decrease was not found to be significant for the brush-like polymers prepared from the ethylene oxide modified surfaces (SF_{EO}–PEG). Using the captive bubble method, SF_{EO}-zwitter and SF_{OX}-zwitter (Fig. 2b) both show a contact angle of approximately 20°, a significant reduction from SF–Br that confirms successful functionalisation. The captive bubble method (Fig. 2b) also shows that the SF_{EO}-zwitter and SF_{OX}-zwitter display significantly lower contact angles than SF_{EO}–PEG and SF_{OX}–PEG.

The changes in the surface morphology of the films were characterised by atomic force microscopy (AFM), and the height micrographs of the modified silks are shown in Fig. 3. SF_{EO} (Fig. 3a) appeared to be more uneven than did the SF_{OX}, but both films modified with the brush-like polymers exhibited increased height when compared to SF_{EO} (Fig. 3e) and SF_{OX} (Fig. 3d), providing further evidence that the polymerisation was successful. Compared to the brush-like polymer films prepared on the surfaces modified with ethylene oxide, the brush-like surfaces prepared from the oxidised surfaces appeared to be more uniform. While both the ethylene oxide and the oxidation reactions led to brush-like polymers on the surface of the silk films, we elected to focus the next series of experiments on the oxidised series of films due to their appearance of uniformity, greater brush-like polymer thickness based on FTIR measurements, and the potential for the future generation of patterned brush-like surfaces by employing masks during the light-catalysed oxidation reaction.

3.2 Beta sheet secondary structure formation

Silk fibroin is known to self-assemble into beta sheet secondary structures.[2,4,79,85] Tuning beta sheet content affords the opportunity to tune SF's properties, including degradation and mechanical properties, therefore we assessed the changes in beta sheet content of the films as they progressed from ''As Cast'' films ($SF_{As\ Cast}$) through the synthesis and processing steps to generate the brush-like surfaces (Table 1). ATR-FTIR scans of all films were measured to analyse the amide I region (1600 to 1700 cm^{-1}), which is known to display spectral changes in response to changing protein structure. For example, peaks that correspond to random coils are positioned at 1650 cm^{-1} and 1540 cm^{-1} transition to 1625 cm^{-1} and 1515 cm^{-1}, respectively.[79] The amide I region was deconvoluted into peaks corresponding to different secondary structures using established methods.[79] Table 1 shows the beta sheet content measured after each reaction, without the application of any other treatments to deliberately trigger the secondary structure, such as exposure to water vapour or methanol. For the EO series, $SF_{As\ Cast}$ exhibited the lowest beta sheet content of all of the films (about 19.7%). The subsequent reactions, the EO treatment and the initiator attachment, do not induce further changes in beta sheet content. This is expected because these reactions do not utilise solvents or other conditions that have been shown to change the conformation of silk. After the DMAPS and PEGMA polymerisations, the beta sheet content increases to approximately 34–35%, which is a result of the exposure of films to methanol during the reaction. In the OX series, the SF_{WVA} films contain more beta sheet content than

Table 1 Beta sheet content of modified SF films through synthesis and modification

	Beta sheet content (%)	
	EO[a]	OX[b]
Unmodified SF	19.7 ± 4.19 (this film is $SF_{As\ Cast}$)	27.5 ± 1.22 (this film is SF_{WVA})
Hydroxylated SF	21.3 ± 3.68	29.0 ± 2.83
SF–Br	24.1 ± 2.35	28.4 ± 3.46
SF-zwitter	35.6 ± 2.99	35.2 ± 3.04
SF–PEG	34.0 ± 3.01	34.5 ± 2.18

[a] Initial modification by ethylene oxide. [b] Initial modification by photocatalysed oxidation.

Table 2 Beta sheet content of modified silk films after exposure to 95 v/v% methanol

	Beta sheet content (%)	
	EO[a]	OX[b]
Hydroxylated SF	34.3 ± 2.74	37.1 ± 3.38
SF-zwitter	36.3 ± 4.44	37.7 ± 3.92
SF–PEG	35.9 ± 2.50	36.5 ± 4.09

[a] Initial modification by ethylene oxide. [b] Initial modification by photocatalysed oxidation.

the $\mathbf{SF_{As\ Cast}}$ films used in the EO series, a finding that is consistent with literature.[19] Similar to the EO series, the surface oxidation and initiator attachment reactions do not induce beta sheets, but the DMAPS and PEGMA polymerisations increase the beta sheet content. Again, this was expected due to the films being exposed to methanol during the polymerisations.

The impact of the brush-like polymer surface modifications on the protein's ability to form beta sheet structures was also quantified. To complete this study, the films in the EO and OX series were first prepared as described above. Each film was then annealed by soaking in 95% methanol in water for 24 h at 25 °C, drying, and then analyzing beta sheet content using ATR-FTIR with peak deconvolution. The goal was to determine if the surface functionalisations affect the final amount of beta sheet that can form. "As Cast" SF films ($\mathbf{SF_{As\ Cast}}$) soaked in the methanol solution under these conditions were found to display 36.7 ± 2.30% beta sheet content. Table 2 shows that the hydroxylated SFs ($\mathbf{SF_{EO}}$ and $\mathbf{SF_{OX}}$) and the SF films with brush-like polymers (**SF-zwitter** and **SF–PEG**) all show beta sheet contents similar to the "As Cast" unmodified SF films, indicating that the surface functionalisation does not affect the ability of the protein film to form beta sheets.

3.3 Film degradation

SF has been shown to degrade *via* hydrolysis or at an accelerated rate by treating with Protease XIV, the rate of which is dependent on its beta sheet content.[19,21,80] It was not known how the degradation would be affected by the brush-like polymer surfaces. Films were exposed to 1 U mL^{-1} protease XIV in 1X PBS (enzyme) (Fig. 4a) or 1X PBS only (control) (Fig. 4b).

$\mathbf{SF_{OX}}$, $\mathbf{SF_{OX}}$**-zwitter**, and $\mathbf{SF_{OX}}$**–PEG** films all show similar degradation profiles. This suggests that the presence of the brush-like polymers, though synthetic, do not hinder the ability of the film to degrade. SF was found to degrade faster and reach a lower mass than the modified films. The slower degradation of the functionalised silk surfaces is attributed to the lack of degradation of the polymer brushes and the decreased ability of the enzyme to attach to the more hydrophilic surfaces. The degradation profiles from incubation in 1X PBS are shown in Fig. 4b, where all compositions show resistance to degradation over the duration of the experiment (14 days). This result is consistent with the literature, where silk fibroin with beta sheet content degrades over much longer timescales without the presence of Protease XIV.[19,21,80,86]

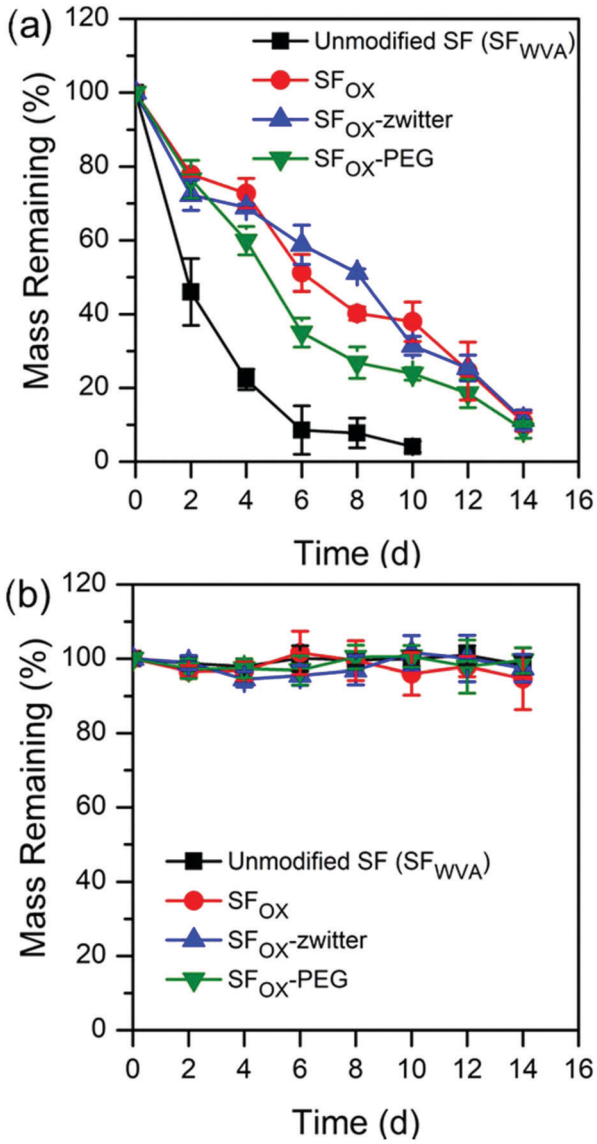

Fig. 4 Degradation profiles of water annealed silk ($\mathbf{SF_{WVA}}$), hydroxylated silk ($\mathbf{SF_{OX}}$), and the silk brush-like polymer films in (a) 1 U mL^{-1} protease XIV and (b) 1X PBS, at 37 °C.

3.4 Protein and cellular attachment studies

To evaluate the biofouling potential of the modified SF films, protein adsorption was quantified. Bovine serum albumin (BSA) was selected for investigation because it is a large component in blood,[87,88] one of the first substances to deposit after a biomaterial is implanted,[89,90] and is the protein that is frequently used as a model foulant, including for applications in marine fouling[91–93] and filtration membranes.[94–96] The films were incubated with a solution of BSA, rinsed with water to remove loosely attached protein, and then treated with a surfactant solution. The surfactant was used to remove bound protein and was assayed to quantify the amount of protein adsorbed onto the surface, which was then divided by the area of the film (9.6 cm^2) to obtain the values reported in Fig. 5. Films that were not exposed to BSA did not result in a detectable amount of protein in the surfactant

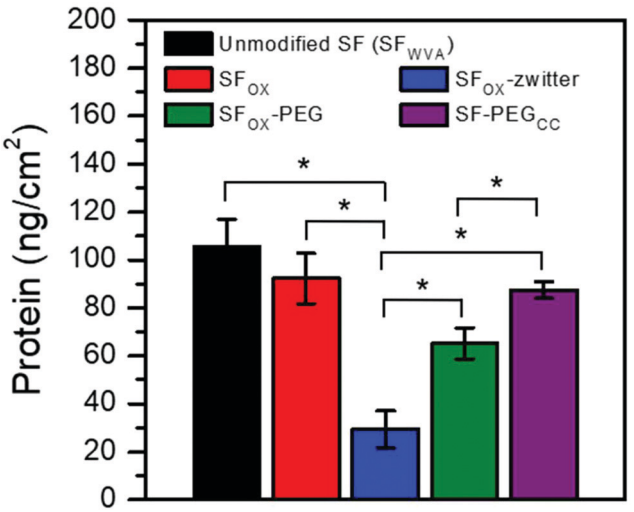

Fig. 5 Amount (ng cm^{-2}) of bovine serum albumin (BSA) adsorbed onto unmodified silk, oxidized silk, and silk brush-like polymer surfaces normalized to film area. * denotes significance at $p < 0.05$.

solution, indicating that the signal from this assay is from the adsorbed BSA and not the release of silk protein from the film. Compared to the water vapour annealed SF (**SF$_{WVA}$**), **SF$_{OX}$** showed a similar amount of BSA bound to the surface, despite the finding that **SF$_{OX}$** displayed a significantly lower contact angle (about 30° by captive bubble) than **SF$_{WVA}$** (about 65° by captive bubble). These results show that, though changes in contact angle may be observed, the addition of hydrophilic functional groups does not necessitate a reduction in protein attachment. The polymer chains "grafted from" the film's surface using ATRP (**SF$_{OX}$-zwitter** and **SF$_{OX}$–PEG**) showed a reduction in the amount of protein adhered to the surface. **SF$_{OX}$-zwitter** showed the lowest amount of BSA adhered to the surface, indicating the zwitterionic brush-like polymers display less fouling than the PEG-containing brush-like polymers. To compare these results to the literature, we replicated a synthesis that conjugated a 5 kDa PEG molecule to silk fibroin surfaces using a "grafting to" method to result in the product **SF–PEG$_{CC}$**. The water contact angles of the surfaces are similar and not statistically different, specifically ~42° for **SF$_{OX}$–PEG** and ~45° for **SF–PEG$_{CC}$**. The molecular weights of the PEG containing chains are also similar: **SF–PEG$_{CC}$** chains are ~5000 g mol^{-1} and **SF$_{OX}$–PEG** chains are ~8000 g mol^{-1} (Table S1, ESI†). The finding that **SF$_{OX}$–PEG** had less protein bound than **SF–PEG$_{CC}$** may be due to several factors. First, there may be a greater density of brush-like polymers on the **SF$_{OX}$–PEG** surfaces compared to **SF–PEG$_{CC}$** because of the use of "grafting from" to synthesize **SF$_{OX}$–PEG.** The chain architecture is also different (**SF–PEG$_{CC}$** has PEG in the backbone and is terminated with a methoxy group, but **SF$_{OX}$–PEG** has PEG pendant groups and is terminated with bromine) and may impact interactions between neighboring chains and the coverage of the film surface. Molecular weight of the chains may also contribute to this difference, but this seems less likely because the chains are both oligomeric and the values are similar to what others have used for polymer brushes. While comparing the outcomes of protein attachment studies reported in literature is somewhat challenging due to differences in methods and how data are reported, the **SF-zwitter** surfaces have protein attachment of ~29.2 ± 7.7 ng cm^{-2}, which is lower than other methods to reduce attachment to SF surfaces. Varying the surface density, molecular weight, and pendant group composition of the brush-like polymers may enable tuning of attachment and is the subject of ongoing work.

Cell attachment to the SF and modified SF films was investigated by seeding human mesenchymal stem cells (hMSCs) onto the films and quantifying the number of cells quantified after incubating for 1 h, 3 h, 6 h, and 24 h. hMSCs were selected for study because they are present in the

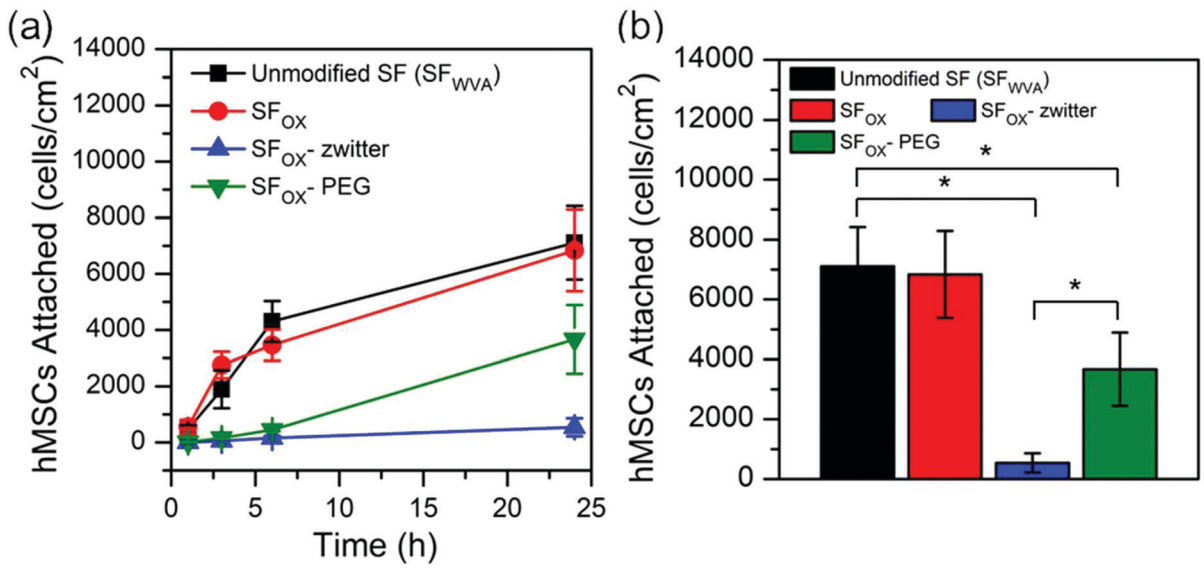

Fig. 6 Attachment (cells per cm^2) of human mesenchymal stem cells (hMSCs) to unmodified silk, oxidized silk, and silk brush-like polymer surfaces normalized to film area at (a) 1 h, 3 h, 6 h, and 24 h; and (b) 24 h. * denotes significance at $p < 0.05$.

circulation and can migrate to wounded areas to start the process of tissue regeneration. The number of cells attached to the samples at each time point and after 24 h are shown in Fig. 6a and b, respectively. A similar number of cells attached to the water vapour annealed silk ($\mathbf{SF_{WVA}}$) and $\mathbf{SF_{OX}}$, illustrating that even though $\mathbf{SF_{OX}}$ is more hydrophilic than **SF**, it is not more effective at repelling attachment of cells, a finding that is consistent with the protein adhesion experiments (Fig. 5). $\mathbf{SF_{OX}}$**–PEG** depicted fewer cells adhered than $\mathbf{SF_{WVA}}$ or $\mathbf{SF_{OX}}$, suggesting that the PEG brush-like polymers are effective at reducing fouling. $\mathbf{SF_{OX}}$**-zwitter** exhibited the lowest number of cells attached, which is consistent with the protein adhesion results and highlights the zwitterionic brush-like polymer surface's resistance to biofouling. The data shown in Fig. 6 is consistent with images of cells seeded on the different films acquired at the 24 h time point (Fig. S5, ESI†). Taken together, the protein and cell adhesion data indicate that both the PEG-containing brush-like polymers and the zwitterionic brush-like polymers are capable of decreasing BSA and hMSC attachment compared to unmodified SF and existing ''grafting to'' methods, but that the zwitterionic compositions lead to greater reductions in attachment. Finally, some literature has noted differences between how cells and protein attach to the polymer-functionalised silk surfaces. For example, in some cases, surface functionalization with polymers reduces cell attachment but not protein attachment, while in other cases, surface functionalisation with polymers reduces attachment of large proteins like antibodies, but not smaller proteins, like albumin. The surfaces prepared and characterized here showed the same trend in cell and protein attachment, which may indicate that the oxidised method yields a greater uniformity in conjugation, greater density of the chains, or perhaps some combination of these and other factors, though this cannot be stated with certainty because the surfaces could not be directly compared.

4. Conclusions

This work successfully functionalised the surfaces of silk fibroin films with hydrophilic and zwitterionic polymer brushes using atom transfer radical polymerisation (ATRP). To polymerise the brushes, initiating molecules were first attached to the films at free hydroxyl groups and then polymer chains were grown from the surfaces using acrylate monomers. Initial experiments that functionalised the surfaces of methanol-annealed silk films were found to result in very little polymer brush attachment, leading to the hypothesis that hydroxyl group accessibility may be reduced by the presence of beta sheet structures. Two different methods were therefore investigated to enrich the surface of the films with hydroxyl groups prior to initiator attachment, where the first method conjugated ethylene oxide and the second method used a two-step oxidation reaction. One advantage of the ethylene oxide reaction is that it does not require silk to be water insoluble, therefore it permits the use of ''As Cast'' films with lower amounts of beta sheet. In contrast, the photo-catalysed oxidation reaction requires a water-insoluble film, but it can generate hydroxyl groups at a large number of reactive sites, including secondary amines along the protein's backbone. Both methods increased film hydrophilicity significantly, as determined by a reduction in contact angle with water.

Initiator was attached to the films and two types of brush-like polymers, one containing a zwitterionic pendant group (DMAPS) and the other containing a poly(ethylene glycol) (PEG) pendant group, were grown from the surfaces using a ''grafting from'' method. AFM micrographs of the brush-like polymer surfaces appear to be more uniform when generated on the oxidised surfaces, and ATR-FTIR suggests that there is a larger amount of the zwitterionic brushlike-polymers on the oxidised surfaces as well. Surfaces functionalised with PEG-containing brush-like polymers were found to display a lower contact angle with water compared to unmodified surfaces, though this was significant only for the oxidised series of films, and brush-like polymers with zwitterionic side chains were found to reduce the contact angle with water to an even larger extent than the PEG-containing polymers. The presence of brush-like polymers slowed, but did not prevent, film degradation.

Albumin is one of the most abundant proteins in serum and deposits quickly to facilitate cellular attachment, therefore the ability of the films to attach BSA was characterised. Surfaces containing PEG ''grafted from'' the film displayed significantly lower protein attachment compared to the control surfaces and the PEG ''grafted to'' surfaces. Zwitterionic brush-like polymers grown from oxidised surfaces displayed significantly lower protein attachment than the methods to prepare PEG brush-like polymers. Human mesenchymal stem cell attachment followed the same trends, where attachment was highest on the control surface, reduced on PEG brush-like polymers prepared by ''grafting from'', and lowest on the zwitterionic brush-like polymer surfaces prepared by ''grafting from''. This work thus reports on new methods to generate brush-like polymer surfaces on silk fibroin and demonstrates the enhanced ability of zwitterionic surfaces to decrease cell and protein attachment compared to uncharged hydrophilic surfaces. Combining the zwitterionic brush chemistry with the photo-catalysed oxidation reaction is expected to permit spatial control over cell and protein attachment to silk biomaterial surfaces and is envisioned to advance the utility of implanted silk materials that require control of diffusion around surfaces, such as drug delivery implants.

Conflicts of interest

There are no conflicts to declare.

Acknowledgements

This work was supported by the University of Connecticut (laboratory start-up funding and the Research Excellence Program Award to KAB) and by the National Science Foundation award to DHA (CHE 2004072). DLH acknowledges the Department of Education

for a Graduate Assistance in Areas of National Need (GAANN) Fellowship (Award P200A150330 and P200A180065).

Notes and references

1 Y. Q. Zhang, Applications of Natural Silk Protein Sericin in Biomaterials, *Biotechnol. Adv.*, 2002, **20**(2), 91–100.
2 C. Vepari and D. L. Kaplan, Silk as a Biomaterial, *Prog. Polym. Sci.*, 2007, **32**(8–9), 991–1007.
3 A. R. Murphy and D. L. Kaplan, Biomedical Applications of Chemically-Modified Silk Fibroin, *J. Mater. Chem.*, 2009, **19**(36), 6443–6450.
4 G. H. Altman, F. Diaz, C. Jakuba, T. Calabro, R. L. Horan, J. Chen, H. Lu, J. Richmond and D. L. Kaplan, Silk-Based Biomaterials, *Biomaterials*, 2003, **24**, 401–416.
5 L. Meinel, R. Fajardo, S. Hofmann, R. Langer, J. Chen, B. Snyder, G. Vunjak-Novakovic and D. Kaplan, Silk Implants for the Healing of Critical Size Bone Defects, *Bone*, 2005, **37**(5), 688–698.
6 Y. Nakazawa, M. Sato, R. Takahashi, D. Aytemiz, C. Takabayashi, T. Tamura, S. Enomoto, M. Sata and T. Asakura, Development of Small-Diameter Vascular Grafts Based on Silk Fibroin Fibers from Bombyx Mori for Vascular Regeneration, *J. Biomater. Sci., Polym. Ed.*, 2011, **22**(1–3), 195–206.
7 G. S. Perrone, G. G. Leisk, T. J. Lo, J. E. Moreau, D. S. Haas, B. J. Papenburg, E. B. Golden, B. P. Partlow, S. E. Fox and A. M. S. Ibrahim, *et al.*, The Use of Silk-Based Devices for Fracture Fixation, *Nat. Commun.*, 2014, **5**, 1–9.
8 Y. Wang, D. J. Blasioli, H. J. Kim, H. S. Kim and D. L. Kaplan, Cartilage Tissue Engineering with Silk Scaffolds and Human Articular Chondrocytes, *Biomaterials*, 2006, **27**(25), 4434–4442.
9 H. Fan, H. Liu, S. L. Toh and J. C. H. Goh, Anterior Cruciate Ligament Regeneration Using Mesenchymal Stem Cells and Silk Scaffold in Large Animal Model, *Biomaterials*, 2009, **30**(28), 4967–4977.
10 B. B. Mandal and S. C. Kundu, Cell Proliferation and Migration in Silk Fibroin 3D Scaffolds, *Biomaterials*, 2009, **30**(15), 2956–2965.
11 J. R. Mauney, T. Nguyen, K. Gillen, C. Kirker-Head, J. M. Gimble and D. L. Kaplan, Engineering Adipose-like Tissue *in Vitro* and *in Vivo* Utilizing Human Bone Marrow and Adipose-Derived Mesenchymal Stem Cells with Silk Fibroin 3D Scaffolds, *Biomaterials*, 2007, **28**(35), 5280–5290.
12 L. P. Yan, J. Silva-Correia, M. B. Oliveira, C. Vilela, H. Pereira, R. A. Sousa, J. F. Mano, A. L. Oliveira, J. M. Oliveira and R. L. Reis, Bilayered Silk/Silk-NanoCaP Scaffolds for Osteochondral Tissue Engineering: In Vitro and in Vivo Assessment of Biological Performance, *Acta Biomater.*, 2015, **12**(1), 227–241.
13 R. D. Abbott, E. P. Kimmerling, D. M. Cairns and D. L. Kaplan, Silk as a Biomaterial to Support Long-Term Three-Dimensional Tissue Cultures, *ACS Appl. Mater. Interfaces*, 2016, **8**(34), 21861–21868.
14 E. Wenk, H. P. Merkle and L. Meinel, Silk Fibroin as a Vehicle for Drug Delivery Applications, *J. Controlled Release*, 2011, **150**(2), 128–141.
15 T. Yucel, M. L. Lovett and D. L. Kaplan, Silk-Based Biomaterials for Sustained Drug Delivery, *J. Controlled Release*, 2014, **190**, 381–397.
16 L. S. Wray, X. Hu, J. Gallego, I. Georgakoudi, F. G. Omenetto, D. Schmidt and D. L. Kaplan, Effect of Processing on Silk-Based Biomaterials: Reproducibility and Biocompatibility, *J. Biomed. Mater. Res., Part A*, 2011, **99 B**(1), 89–101.
17 B. P. Partlow, C. W. Hanna, J. Rnjak-Kovacina, J. E. Moreau, M. B. Applegate, K. A. Burke, B. Marelli, A. N. Mitropoulos, F. G. Omenetto and D. L. Kaplan, Highly Tunable Elastomeric Silk Biomaterials, *Adv. Funct. Mater.*, 2014, **24**(29), 4615–4624.
18 B. P. Partlow, A. P. Tabatabai, G. G. Leisk, P. Cebe, D. L. Blair and D. L. Kaplan, Silk Fibroin Degradation Related to Rheological and Mechanical Properties, *Macromol. Biosci.*, 2016, **16**(5), 666–675.
19 X. Hu, K. Shmelev, L. Sun, E.-S. Gil, S.-H. Park, P. Cebe and D. L. Kaplan, Regulation of Silk Material Structure by Temperature-Controlled Water Vapor Annealing, *Biomacromolecules*, 2011, **12**(5), 1686–1696.
20 C. Jiang, X. Wang, R. Gunawidjaja, Y. H. Lin, M. K. Gupta, D. L. Kaplan, R. R. Naik and V. V. Tsukruk, Mechanical Properties of Robust Ultrathin Silk Fibroin Films, *Adv. Funct. Mater.*, 2007, **17**(13), 2229–2237.
21 Q. Lu, B. Zhang, M. Li, B. Zuo, D. L. Kaplan, Y. Huang and H. Zhu, Degradation Mechanism and Control of Silk Fibroin, *Biomacromolecules*, 2011, **12**(4), 1080–1086.
22 A. E. Terry, D. P. Knight, D. Porter and F. Vollrath, PH Induced Changes in the Rheology of Silk Fibroin Solution from the Middle Division of Bombyx Mori Silkworm, *Biomacromolecules*, 2004, **5**(3), 768–772.
23 U. J. Kim, J. Park, C. Li, H. J. Jin, R. Valluzzi and D. L. Kaplan, Structure and Properties of Silk Hydrogels, *Biomacromolecules*, 2004, **5**(3), 786–792.
24 S. Nagarkar, A. Patil, A. Lele, S. Bhat, J. Bellare and R. A. Mashelkar, Some Mechanistic Insights into the Gelation of Regenerated Silk Fibroin Sol, *Ind. Eng. Chem. Res.*, 2009, **48**(17), 8014–8023.
25 X. Wang, J. A. Kluge, G. G. Leisk and D. L. Kaplan, Sonication-Induced Gelation of Silk Fibroin for Cell Encapsulation, *Biomaterials*, 2008, **29**(8), 1054–1064.
26 X. Hu, Q. Lu, L. Sun, P. Cebe, X. Wang, X. Zhang and D. L. Kaplan, Biomaterials from Ultrasonication-Induced Silk Fibroin-Hyaluronic Acid Hydrogels, *Biomacromolecules*, 2010, **11**(11), 3178–3188.
27 T. Yucel, P. Cebe and D. L. Kaplan, Vortex-Induced Injectable Silk Fibroin Hydrogels, *Biophys. J.*, 2009, **97**(7), 2044–2050.
28 M. Ishida, T. Asakura, M. Yokoi and H. Saito, Solvent- and Mechanical-Treatment-Induced Conformational Transjtion of Silk Fibroins Studied by High-Resolution Solid-State 13C NMR Spectroscopy, *Macromolecules*, 1990, **23**(1), 88–94.
29 M. Canetti, A. Seves, F. Secundo and G. Vecchio, CD and Small-angle X-ray Scattering of Silk Fibroin in Solution, *Biopolymers*, 1989, **28**(9), 1613–1624.
30 C.-Z. Zhou, F. Confalonieri, M. Jacquet, R. Perasso, Z.-G. Li and J. Janin, Silk Fibroin: Structural Implications of a

Remarkable Amino Acid Sequence, *Proteins: Struct., Funct., Genet.*, 2001, **44**(2), 119–122.

31 T. Asakura, R. Sugino, J. Yao, H. Takashima and R. Kishore, Comparative Structure Analysis of Tyrosine and Valine Residues in Unprocessed Silk Fibroin (Silk I) and in the Processed Silk Fiber (Silk II) from Bombyx Mori Using Solid-State ^{13}C,^{15}N, and 2H NMR, *Biochemistry*, 2002, **41**(13), 4415–4424.

32 E. Bini, D. P. Knight and D. L. Kaplan, Mapping Domain Structures in Silks from Insects and Spiders Related to Protein Assembly, *J. Mol. Biol.*, 2004, **335**, 27–40.

33 Y. Tamada, Sulfation of Silk Fibroin by Chlorosulfonic Acid and the Anticoagulant Activity, *Biomaterials*, 2004, **25**(3), 377–383.

34 S. Wang, Z. Gao, X. Chen, X. Lian, H. Zhu, J. Zheng and L. Sun, The Anticoagulant Ability of Ferulic Acid and Its Applications for Improving the Blood Compatibility of Silk Fibroin, *Biomed. Mater.*, 2008, **3**, 4.

35 E. Fournier, C. Passirani, C. N. Montero-Menei and J. P. Benoit, Biocompatibility of Implantable Synthetic Polymeric Drug Carriers: Focus on Brain Biocompatibility, *Biomaterials*, 2003, **24**(19), 3311–3331.

36 L. Kessler, M. Pinget, M. Aprahamian, P. Dejardin and C. Damge, *In Vitro* and *in Vivo* Studies of the Properties of an Artificial Membrane for Pancreatic Islet Encapsulation, *Horm. Metab. Res.*, 1991, **23**(7), 312–317.

37 W. Arung, M. Meurisse and O. Detry, Pathophysiology and Prevention of Postoperative Peritoneal Adhesions, *World J. Gastroenterol.*, 2011, **17**(41), 4545–4553.

38 B. Schnriger, G. Barmparas, B. C. Branco, T. Lustenberger, K. Inaba and D. Demetriades, Prevention of Postoperative Peritoneal Adhesions: A Review of the Literature, *Am. J. Surg.*, 2011, **201**(1), 111–121.

39 C. Vepari, D. Matheson, L. Drummy, R. Naik and D. L. Kaplan, Surface Modification of Silk Fibroin with Poly(Ethylene Glycol) for Antiadhesion and Antithrombotic Applications, *J. Biomed. Mater. Res., Part A*, 2010, **93**(2), 595–606.

40 T. Furuzono, K. Ishihara, N. Nakabayashi and Y. Tamada, Chemical Modification of Silk Fibroin with 2-Methacryloyloxyethyl Phosphorylcholine. II. Graft-Polymerization onto Fabric through 2-Methacryloyloxyethyl Isocyanate and Interaction between Fabric and Platelets, *Biomaterials*, 2000, **21**(4), 327–333.

41 E. Ostuni, R. G. Chapman, R. E. Holmlin, S. Takayama and G. M. Whitesides, A Survey of Structure-Property Relationships of Surfaces That Resist the Adsorption of Protein, *Langmuir*, 2001, **17**(18), 5605–5620.

42 S. Herrwerth, W. Eck, S. Reinhardt and M. Grunze, Factors That Determine the Protein Resistance of Oligoether Self-Assembled Monolayers - Internal Hydrophilicity, Terminal Hydrophilicity, and Lateral Packing Density, *J. Am. Chem. Soc.*, 2003, **125**(31), 9359–9366.

43 C. R. Jenney and J. M. Anderson, Effects of Surface-Coupled Polyethylene Oxide on Human Macrophage Adhesion and Foreign Body Giant Cell Formation in Vitro, *J. Biomed. Mater. Res.*, 1999, **44**(2), 206–216.

44 C. R. Deible, P. Petrosko, P. C. Johnson, E. J. Beckman, A. J. Russell and W. R. Wagner, Molecular Barriers to Biomaterial Thrombosis by Modification of Surface Proteins with Polyethylene Glycol, *Biomaterials*, 1999, **20**(2), 101–109.

45 T. McPherson, A. Kidane, I. Szleifer and K. Park, Prevention of Protein Adsorption by Tethered Poly(Ethylene Oxide) Layers: Experiments and Single-Chain Mean-Field Analysis, *Langmuir*, 1998, **14**(1), 176–186.

46 Z. Zhang, M. Zhang, S. Chen, T. A. Horbett, B. D. Ratner and S. Jiang, Blood Compatibility of Surfaces with Superlow Protein Adsorption, *Biomaterials*, 2008, **29**(32), 4285–4291.

47 L. Bekale, D. Agudelo and H. A. Tajmir-Riahi, The Role of Polymer Size and Hydrophobic End-Group in PEG-Protein Interaction, *Colloids Surf., B*, 2015, **130**, 141–148.

48 M. Shen, L. Martinson, M. S. Wagner, D. G. Castner, B. D. Ratner and T. A. Horbett, PEO-like Plasma Polymerized Tetraglyme Surface Interactions with Leukocytes and Proteins: *In Vitro* and *in Vivo* Studies, *J. Biomater. Sci., Polym. Ed.*, 2002, **13**(4), 367–390.

49 D. A. Herold, K. Keil and D. E. Bruns, Oxidation of Polyethylene Glycols by Alcohol Dehydrogenase, *Biochem. Pharmacol.*, 1989, **38**(1), 73–76.

50 M. He, K. Gao, L. Zhou, Z. Jiao, M. Wu, J. Cao, X. You, Z. Cai, Y. Su and Z. Jiang, Zwitterionic Materials for Antifouling Membrane Surface Construction, *Acta Biomater.*, 2016, **40**(92), 142–152.

51 J. B. Schlenoff, Zwitteration: Coating Surfaces with Zwitterionic Functionality to Reduce Nonspecific Adsorption, *Langmuir*, 2014, **30**(32), 9625–9636.

52 Z. Zhang, J. A. Finlay, L. Wang, Y. Gao, J. A. Callow, M. E. Callow and S. Jiang, Polysulfobetaine-Grafted Surfaces as Environmentally Benign Ultralow Fouling Marine Coatings, *Langmuir*, 2009, **25**(23), 13516–13521.

53 N. Aldred, G. Li, Y. Gao, A. S. Clare and S. Jiang, Modulation of Barnacle (Balanus Amphitrite Darwin) Cyprid Settlement Behavior by Sulfobetaine and Carboxybetaine Methacrylate Polymer Coatings, *Biofouling*, 2010, **26**(6), 673–683.

54 S. Sampaio, T. M. R. Miranda, J. G. Santos and G. M. B. Soares, Preparation of Silk Fibroin-Poly(Ethylene Glycol) Conjugate Films through Click Chemistry, *Polym. Int.*, 2011, **60**(12), 1737–1744.

55 S. Wang, Y. Zhang, H. Wang and Z. Dong, Preparation, Characterization and Biocompatibility of Electrospinning Heparin-Modified Silk Fibroin Nanofibers, *Int. J. Biol. Macromol.*, 2011, **48**(2), 345–353.

56 M. A. Serban and D. L. Kaplan, PH-Sensitive Ionomeric Particles Obtained via Chemical Conjugation of Silk with Poly(Amino Acid)S, *Biomacromolecules*, 2010, **11**(12), 3406–3412.

57 C. Ye, I. Drachuk, R. Calabrese, H. Dai, D. L. Kaplan and V. V. Tsukruk, Permeability and Micromechanical Properties of Silk Ionomer Microcapsules, *Langmuir*, 2012, **28**(33), 12235–12244.

58 S. Das, D. Pati, N. Tiwari, A. Nisal and S. Sen Gupta, Synthesis of Silk Fibroin-Glycopolypeptide Conjugates and Their Recognition with Lectin, *Biomacromolecules*, 2012, **13**(11), 3695–3702.

59 M. R. Buga, C. Zaharia, M. Belan, C. Bressy, F. Ziarelli and A. Margaillan, Surface Modification of Silk Fibroin Fibers with Poly(Methyl Methacrylate) and Poly(Tributylsilyl Methacrylate) via RAFT Polymerization for Marine Antifouling Applications, *Mater. Sci. Eng., C*, 2015, **51**, 233–241.

60 V. Dhyani and N. Singh, Controlling the Cell Adhesion Property of Silk Films by Graft Polymerization, *ACS Appl. Mater. Interfaces*, 2014, **6**(7), 5005–5011.

61 J. Prachayawarakorn and K. Boonsawat, Physical, Chemical, and Dyeing Properties of Bombyx Mori Silks Grafted by 2-hydroxyethyl Methacrylate and Methyl Methacrylate, *J. Appl. Polym. Sci.*, 2007, **106**(3), 1526–1534.

62 G. Freddi, M. R. Massafra, S. Beretta, S. Shibata, Y. Gotoh, H. Yasui and M. Tsukada, Structure and Properties of Bombyx Mori Silk Fibers Grafted with Methacrylamide (MAA) and 2-hydroxyethyl Methacrylate (HEMA), *J. Appl. Polym. Sci.*, 1996, **60**(11), 1867–1876.

63 Y. Sun, Z. Shao, J. Zhou and T. Yu, Compatibilization of Acrylic Polymer–Silk Fibroin Blend Fibers. I. Graft Copolymerzation of Acrylonitrile onto Silk Fibroin, *J. Appl. Polym. Sci.*, 1998, **69**(6), 1089–1097.

64 M. Tsukada, T. Yamamoto, N. Nakabayashi, H. Ishikawa and G. Freddi, Grafting of Methyl Methacrylate onto Silk Fibers Initiated by Tri-*n*-butylborane, *J. Appl. Polym. Sci.*, 1991, **43**(11), 2115–2121.

65 J. Yang, S. Lu, T. Xing and G. Chen, Preparation, Structure, and Properties of Silk Fabric Grafted with 2-Hydroxypropyl Methacrylate Using the HRP Biocatalyzed ATRP Method, *Polymers*, 2018, **10**, 5.

66 T. Xing, H. Wang, L. Zhanxiong and G. Chen, Surface Grafting Modification of Silk Fibroin by Atom Transfer Radical Polymerization, *Key Eng. Mater.*, 2008, **373–374**, 629–632.

67 S. Li, T. Xing, Z. Li and G. Chen, Structure and Properties of Silk Grafted with Acrylate Fluoride Monomers by ATRP, *Appl. Surf. Sci.*, 2013, **268**, 92–97.

68 T. Xing, W. Hu, S. Li and G. Chen, Preparation, Structure and Properties of Multi-Functional Silk via ATRP Method, *Appl. Surf. Sci.*, 2012, **258**(7), 3208–3213.

69 R. Barbey, L. Lavanant, D. Paripovic, N. Schüwer, C. Sugnaux, S. Tugulu and H. A. Klok, Polymer Brushes via Surface-Initiated Controlled Radical Polymerization: Synthesis, Characterization, Properties, and Applications, *Chem. Rev.*, 2009, **109**(11), 5437–5527.

70 P. Taddei, M. Di Foggia, S. Martinotti, E. Ranzato, I. Carmagnola, V. Chiono and M. Tsukada, Silk Fibres Grafted with 2-Hydroxyethyl Methacrylate (HEMA) and 4-Hydroxybutyl Acrylate (HBA) for Biomedical Applications, *Int. J. Biol. Macromol.*, 2018, **107**(PartA), 537–548.

71 T. Furuzono, K. Ishihara, N. Nakabayashi and Y. Tamada, Chemical Modification of Silk Fibroin with 2-Methacryloyloxyethyl Phosphorylcholine. II. Graft-Polymerization onto Fabric through 2-Methacryloyloxyethyl Isocyanate and Interaction between Fabric and Platelets, *Biomaterials*, 2000, **21**(4), 327–333.

72 Y. Jiang, H. Qingfeng, L. Baolei, S. Jian and L. Sicong, Platelet Adhesive Resistance of Polyurethane Surface Grafted with Zwitterions of Sulfobetaine, *Colloids Surf., B*, 2004, **36**(1), 19–26.

73 J. Huang and W. Xu, Zwitterionic Monomer Graft Copolymerization onto Polyurethane Surface through a PEG Spacer, *Appl. Surf. Sci.*, 2010, **256**(12), 3921–3927.

74 L. Zhang, Z. Cao, T. Bai, L. Carr, J. R. Ella-Menye, C. Irvin, B. D. Ratner and S. Jiang, Zwitterionic Hydrogels Implanted in Mice Resist the Foreign-Body Reaction, *Nat. Biotechnol.*, 2013, **31**(6), 553–556.

75 X. Jiang, Q. Chen, S. Lin and J. Shen, Surface Modification of Silk Fibroin Films with Zwitterionic Phosphobetaine to Improve the Hemocompatibility, *J. Wuhan Univ. Technol., Mater. Sci. Ed.*, 2010, **25**(6), 969–974.

76 D. A. Wang, C. G. Williams, Q. Li, B. Sharma and J. H. Elisseeff, Synthesis and Characterization of a Novel Degradable Phosphate-Containing Hydrogel, *Biomaterials*, 2003, **24**(22), 3969–3980.

77 D. N. Rockwood, R. C. Preda, T. Yucel, X. Wang, M. L. Lovett and D. L. Kaplan, Materials Fabrication from Bombyx Mori Silk Fibroin, *Nat. Protoc.*, 2011, **6**, 1612–1631.

78 P. Yang, J. Y. Deng and W. T. Yang, Confined Photo-Catalytic Oxidation: A Fast Surface Hydrophilic Modification Method for Polymeric Materials, *Polymer*, 2003, **44**(23), 7157–7164.

79 X. Hu, D. Kaplan and P. Cebe, Determining Beta Sheet Crystallinity in Fibrous Proteins by Thermal Analysis and Infrared Spectroscopy, *Macromolecules*, 2006, **39**, 6161–6170.

80 R. L. Horan, K. Antle, A. L. Collette, Y. Wang, J. Huang, J. E. Moreau, V. Volloch, D. L. Kaplan and G. H. Altman, *In Vitro* Degradation of Silk Fibroin, *Biomaterials*, 2005, **26**(17), 3385–3393.

81 H. J. Jin, J. Park, V. Karageorgiou, U. J. Kim, R. Valluzzi, P. Cebe and D. L. Kaplan, Water-Stable Silk Films with Reduced β-Sheet Content, *Adv. Funct. Mater.*, 2005, **15**(8), 1241–1247.

82 K. S. Hu, A. I. Darer and M. J. Elrod, Thermodynamics and Kinetics of the Hydrolysis of Atmospherically Relevant Organonitrates and Organosulfates, *Atmos. Chem. Phys.*, 2011, **11**(16), 8307–8320.

83 Di. A. Cortés and M. J. Elrod, Kinetics of the Aqueous Phase Reactions of Atmospherically Relevant Monoterpene Epoxides, *J. Phys. Chem. A*, 2017, **121**(48), 9297–9305.

84 S. Bing, J. Wang, H. Xu, Y. Zhao, Y. Zhou, L. Zhang, C. Gao and L. Hou, Polyamide Thin-Film Composite Membrane Modified with Persulfate for Improvement of Perm-Selectivity and Chlorine-Resistance, *J. Membr. Sci.*, 2018, **555**(November 2017), 318–326.

85 A. Matsumoto, J. Chen, A. L. Collette, U. J. Kim, G. H. Altman, P. Cebe and D. L. Kaplan, Mechanisms of Silk Fibroin Sol-Gel Transitions, *J. Phys. Chem. B*, 2006, **110**(43), 21630–21638.

86 M. Li, M. Ogiso and N. Minoura, Enzymatic Degradation Behavior of Porous Silk Fibroin Sheets, *Biomaterials*, 2003, **24**(2), 357–365.

87 K. A. Majorek, P. J. Porebski, A. Dayal, M. D. Zimmerman, K. Jablonska, A. J. Stewart, M. Chruszcz and W. Minor,

Structural and Immunologic Characterization of Bovine, Horse, and Rabbit Serum Albumins, *Mol. Immunol.*, 2012, **52**(3–4), 174–182.

88 J. E. Hall, *Guyton and Hall Textbook of Medical Physiology*, Elsevier Inc., Philadelphia, PA, 13th edn, 2016.

89 W. G. Pitt, K. Park and S. L. Cooper, Sequential Protein Adsorption and Thrombus Deposition on Polymeric Biomaterials, *J. Colloid Interface Sci.*, 1986, **111**(2), 343–362.

90 B. D. Ratner and S. J. Bryant, Biomaterials: Where We Have Been and Where We Are Going, *Annu. Rev. Biomed. Eng.*, 2004, **6**(1), 41–75.

91 C. S. Gudipati, J. A. Finlay, J. A. Callow, M. E. Callow and K. L. Wooley, The Antifouling and Fouling-Release Perfomance of Hyperbranched Fluoropolymer (HBFP)–Poly(Ethylene Glycol) (PEG) Composite Coatings Evaluated by Adsorption of Biomacromolecules and the Green Fouling Alga Ulva, *Langmuir*, 2005, **21**(7), 3044–3053.

92 W. J. Yang, K. G. Neoh, E. T. Kang, S. S. C. Lee, S. L. M. Teo and D. Rittschof, Functional Polymer Brushes *via* Surface-Initiated Atom Transfer Radical Graft Polymerization for Combating Marine Biofouling, *Biofouling*, 2012, **28**(9), 895–912.

93 K. A. Pollack, P. M. Imbesi, J. E. Raymond and K. L. Wooley, Hyperbranched Fluoropolymer-Polydimethylsiloxane-Poly (Ethylene Glycol) Cross-Linked Terpolymer Networks Designed for Marine and Biomedical Applications: Heterogeneous Non-toxic Antibiofouling Surfaces, *ACS Appl. Mater. Interfaces*, 2014, **6**(21), 19265–19274.

94 A. Asatekin, A. Menniti, S. Kang, M. Elimelech, E. Morgenroth and A. M. Mayes, Antifouling Nanofiltration Membranes for Membrane Bioreactors from Self-Assembling Graft Copolymers, *J. Memb. Sci.*, 2006, **285**(1–2), 81–89.

95 X. Li, R. Pang, J. Li, X. Sun, J. Shen, W. Han and L. Wang, *In Situ* Formation of Ag Nanoparticles in PVDF Ultrafiltration Membrane to Mitigate Organic and Bacterial Fouling, *Desalination*, 2013, **324**, 48–56.

96 G. Xu, P. Liu, D. Pranantyo, L. Xu, K. G. Neoh and E. T. Kang, Antifouling and Antimicrobial Coatings from Zwitterionic and Cationic Binary Polymer Brushes Assembled via "Click" Reactions, *Ind. Eng. Chem. Res.*, 2017, **56**(49), 14479–14488.

